

UC Berkeley

UC Berkeley Previously Published Works

Title

Se Isotopes as Groundwater Redox Indicators: Detecting Natural Attenuation of Se at an in Situ Recovery U Mine

Permalink

<https://escholarship.org/uc/item/2kr0324w>

Journal

Environmental Science and Technology, 50(20)

ISSN

0013-936X

Authors

Basu, Anirban
Schilling, Kathrin
Brown, Shaun T
[et al.](#)

Publication Date

2016-10-18

DOI

10.1021/acs.est.6b01464

Peer reviewed

17*Corresponding author: E-mail: anirbanbasu@berkeley.edu; phone: (510) 643 5062; fax: (510) 642 9520

18#Authors contributed equally to this manuscript.

19ABSTRACT

20One of the major ecological concerns associated with in situ recovery (ISR) of uranium is the
21environmental release of soluble, toxic Se-oxyanions generated by mining. Post-mining natural
22attenuation by the residual reductants in the ore body and reduced downgradient sediments
23should mitigate the risk of Se contamination in groundwater. In this work, we investigate the Se
24concentrations and Se isotope systematics of groundwater and of U ore bearing sediments from
25an ISR site at Rosita, TX, USA. Our results show that selenate (Se(VI)) is the dominant Se
26species in Rosita groundwater, and while several upgradient wells have elevated Se(VI), the
27majority of the ore zone and downgradient wells have little or no Se-oxyanions. In addition, the
28 $\delta^{82}\text{Se}_{\text{VI}}$ of Rosita groundwater is generally elevated relative to the U ore up to +6.14‰, with the
29most enriched values observed in the ore zone wells. Increasing $\delta^{82}\text{Se}$ with decreasing Se(VI)
30conforms to a Rayleigh-type distillation model with an ϵ of $-2.25\text{‰} \pm 0.61\text{‰}$ suggesting natural
31Se(VI) reduction occurring along the hydraulic gradient at the Rosita ISR site. Furthermore, our
32results show that Se isotopes may indicate the onset of U(VI) reduction and thus are excellent
33sensors for detecting and monitoring postmining natural attenuation of both Se oxyanions and
34U(VI) at ISR sites.

35Introduction

36 Information about key reactions and reaction kinetics in redox-interface mineral deposits is
37crucial for understanding ore deposition mechanisms as well as possible remediation-restoration
38strategies. Reductive immobilization of Se is an important reaction that tends to concentrate Se
39in roll-front type ore deposits forming at redox interfaces in groundwater systems^{1,2}. The
40similarity between the redox potential for reduction of Se oxyanions and dissolved hexavalent
41uranium (U(VI)) leads to co-precipitation of Se-minerals and U minerals (Figure 1). Commonly,
42ferroselite (FeSe_2) and pyrite are host minerals for Se in these U ore deposits¹⁻⁴. Compared to its
43average crustal concentration (0.05 mg/kg), high concentrations of Se ranging from 0.5 - 500
44mg/kg are reported from the roll-front deposits in Wyoming, Montana, and Utah in the United
45States⁵⁻⁷. These anomalously high Se concentrations have been used for uranium prospecting,
46particularly to characterize the location and shape of roll-front type deposits⁸.

47 The oxidative dissolution of U ore enriched with Se minerals mobilizes Se and U in the
48groundwater in their toxic, oxidized forms. Se in the effluent from a traditional U mining and
49milling operation in northern Saskatchewan, Canada, led to accumulation of toxic levels of Se in
50aquatic organisms^{9,10}. Elevated Se concentrations in runoff or aquifers are reported from the
51regions of U mining and milling in the USA (e.g., Puerco River, Arizona; New Mexico; Rifle,
52CO)^{11,12}. At present, almost all recent U mining in the USA and ~50% of global U mining
53employs a mining technique known as in situ recovery (ISR) that extracts U by oxidative
54dissolution of roll-front type sandstone-hosted ore deposits^{13,14}. Despite several advantages such
55as the lack of mill tailings and radioactive dust, and its low CO₂ emission footprint, this mining
56method releases Se as toxic, mobile Se oxyanions along with U(VI) directly into groundwater¹⁵.

57 Current strategies to mitigate Se(VI) in the groundwater after the completion of mining include
58 groundwater sweep and occasionally active remediation by biostimulation or injection of abiotic
59 reductants¹⁶.

60 Natural attenuation of U(VI) by the existing reducing environments downgradient of the redox
61 interface at roll-front deposits has been proposed as an inexpensive but effective remediation
62 strategy. Recent work from our group demonstrates conditions favorable for post-mining U(VI)
63 reduction at ISR sites¹⁷ (Add Brown et al., 2015). After the cessation of mining, the residual
64 reducing capacity of the U ore and the prevailing reducing environments downgradient of the ore
65 should reduce mine-generated elevated concentrations of toxic Se oxyanions. The redox potential
66 (Eh) required for the reduction of Se oxyanions is slightly higher than that of U¹⁸⁻²⁰, meaning that
67 the reduction of Se(VI) and/or Se(IV) should precede U(VI) reduction. Therefore, natural
68 attenuation of Se may be an excellent indicator that a system is approaching U(VI) reducing
69 conditions. The challenge is to identify the active reduction of Se in the ore zone and/or
70 downgradient groundwater and distinguish reduction from other processes that may affect
71 aqueous Se concentration such as sorption and dilution.

72 An effective approach to better understand important reactions and possibly the reactions
73 kinetics is the study of variations in stable isotope ratios. Se reduction can be detected by shifts
74 in the relative abundance of its stable isotopes (⁸²Se, ⁸⁰Se, ⁷⁸Se, ⁷⁷Se, ⁷⁶Se, ⁷⁴Se). The reduction of
75 Se(VI) to Se(0) or Se(-II) via the intermediate product Se(IV) induces a kinetic isotopic
76 fractionation resulting in the enrichment of heavier isotopes (i.e., ⁸²Se) in the remaining dissolved
77 Se oxyanions²⁰⁻²³. This enrichment is described in terms of an isotopic enrichment factor ϵ , a per
78 mil quantity, expressed as

79 $\epsilon = 1000\text{‰} * (\alpha - 1)$ (1)

80 where α is the isotopic fractionation factor, defined as $\alpha = \frac{R_{product}}{R_{reactant}}$, where $R_{product}$ and
81 $R_{reactant}$ are the $^{82}\text{Se}/^{76}\text{Se}$ ratios in the reduction product and remaining Se oxyanions,
82 respectively. Relatively large isotopic fractionation factors are observed during microbial
83 reduction of Se(VI) to Se(IV) ($\epsilon \sim -8\text{‰}$) and of Se(IV) to elemental Se ($\epsilon \sim -14\text{‰}$)²⁴. Abiotic
84 reduction of Se(VI) by green rust or of Se(IV) by FeS also induces large fractionations (up to
85 -11‰)^{21,22,25}. In contrast, adsorption of Se(IV) to mineral surfaces results in a smaller
86 fractionation ($\sim -1\text{‰}$)^{25,26}. Thus, Se stable isotope ratios in groundwater are a more reliable
87 indicator of reduction of Se-oxyanions than aqueous concentrations of the Se species, which are
88 less easy to interpret because of the effects of dilution, removal by adsorption, or advection of
89 heterogeneous plumes past sampling points.

90 In this article, we present species-specific Se concentrations and isotopic measurement data for
91 U ore and 33 groundwater samples collected from wells located upgradient, within and
92 downgradient of a roll-front deposit located at an ISR site at Rosita, TX, USA. Sample locations
93 include both previously mined and unmined parts of the site. To our knowledge, this is the first
94 report of Se isotope measurements in groundwater samples across a groundwater redox interface.
95 Here, we demonstrate Se-oxyanion reduction at the site using Se isotope ratios of groundwater,
96 and argue that Se isotopes are sensitive tracers for detecting the onset of naturally occurring
97 U(VI) reduction.

98 **Materials and Methods**

99 **Site description and Groundwater Sampling.** The study site is located at Rosita, TX, USA
100 (Figure 2). A detailed description of the site can be found in ref 17. Briefly, the U roll front

101 deposit at this ISR site is defined by a poorly consolidated, mineralized sand unit bounded above
102 and below by low permeability clay units. For ISR mining, site groundwater fortified with O_2
103 and H_2O_2 was injected into the ore zone in 3 mining units or production area authorizations
104 (PAA) to oxidize and dissolve the U ore utilizing the high natural bicarbonate concentrations to
105 stabilize U- CO_3 complexes. The mining unit PAA 4 has a complete set of monitoring wells but
106 no mining has occurred to date. The mining was followed by a restoration process, except in the
107 most recently mined PAA 3, where the site groundwater treated by reverse osmosis was injected
108 back into the aquifer. A network of existing wells, drilled within, upgradient and downgradient
109 of the ore body, was used for postmining monitoring of the site.

110 Groundwater samples were collected from 33 wells along transects roughly parallel to the
111 current groundwater flow direction. The wells were purged prior to sampling, and samples for
112 Se-oxyanion concentrations and Se isotopes were filtered using 0.45 μm in-line filters and
113 collected in pre-cleaned HDPE bottles with no headspace and no preservatives. The samples
114 were stored at 4 $^{\circ}C$ prior to analysis.

115 **Sediment digestion.** U ore samples were obtained from a borehole adjacent to BL 39 in PAA
1164 (Figure 2). For Se concentration and isotopic analysis, 1.0 g aliquots of sediment samples from
1177 discreet depths were digested in an acid mixture (concentrated HCl + concentrated HNO_3 , 3:1
118 v/v). First, each 1.0 g aliquot was treated with 4 mL of ~ 7 M HNO_3 in Teflon beakers at 80 $^{\circ}C$
119 for about 12 hrs to remove any carbonate from the sediments. The remaining HNO_3 was then
120 evaporated to near dryness at 60 $^{\circ}C$ prior to addition of a freshly prepared acid mixture of HCl
121 and HNO_3 . The samples were digested at 80 $^{\circ}C$ for 24 hr. After digestion, the acid mixture was

122 removed by evaporating to near dryness at 70 °C, and 5 mL of 0.1 N HCl was added. This
123 solution was filtered using 0.45 µm PTFE filters to remove undigested particles.

124 **Sample Purification and Mass Spectrometry.** Se isotope ratios were measured using multi-
125 collector inductively coupled plasma mass spectrometry (MC- ICP-MS) at the Department of
126 Geology, University of Illinois, Urbana-Champaign following the methods described in [refs](#)
127 [27,28](#). For isotopic measurements, we used a double spike technique ($^{74}\text{Se} + ^{77}\text{Se}$) to correct for
128 the isotopic fractionation during mass spectrometry, and any that might occur during sample
129 purification by ion-exchange chromatography. An aliquot of the double spike solution of
130 appropriate species (either Se(IV) or Se(VI)) was added to a carefully weighed aliquot of the
131 sample (groundwater, or digested U ore) containing approximately 100 ng of Se.

132 The Se-oxyanion species was purified from other Se species and matrix elements by ion
133 exchange chromatography²⁸. For the separation of Se(VI), the samples were first acidified with
134 HCl to a final strength not exceeding 0.1 M HCl. The acidified samples were passed through the
135 anion exchange resin (Eichrom Technologies, LLC) where Se(VI) was adsorbed onto the resin
136 while Se(IV) and other matrix elements (e.g., As, Ge) were rinsed out by 0.1 M HCl. Se(VI) was
137 eluted from the resin by 6M HCl and heated to 105 °C for 1 hr. Finally, the samples were diluted
138 to 2 M HCl, sparged with N₂ to remove a volatile Br species, and equilibrated with Kr in the air
139 for 12 hr prior to isotopic analysis.

140 For Se(IV) extraction, the samples were not acidified before loading on the anion exchange
141 resin. The Se(VI) was adsorbed onto the resin and the effluent containing Se(IV) was collected
142 by rinsing with 0.1 M HCl, then oxidized to Se(VI) by treatment with K₂S₂O₈ at 100 °C for 1 hr.
143 After oxidation, all samples were purified using the above procedure for Se(VI) purification.

144 For purification of Se from the digested U ore (as Se(IV)), we first evaporated the samples to
 145 near dryness and then re-dissolved them in 5 mL 0.1 M HCl. An aliquot of this solution
 146 containing ~ 100 ng Se was brought to a strength of 4-6 M HCl prior to purification by hydride
 147 generation described in ref 29. The H₂Se was trapped in a mixture of NaOH and H₂O₂ and
 148 converted to Se(VI). The excess H₂O₂ was removed from the samples by heating (~ 100 °C) prior
 149 to purification using the procedure for Se(VI) described above.

150 Se isotope ratios are reported as δ⁸²Se, a per mil quantity, defined as

$$\begin{aligned}
 & \frac{{}^{82}\text{Se} / {}^{76}\text{Se}_{\text{sample}}}{{}^{82}\text{Se} / {}^{76}\text{Se}_{\text{SRM 3149}}} \\
 & \times 1000 \text{‰} \\
 & \delta^{82}\text{Se} = \text{‰}
 \end{aligned}
 \tag{2}$$

152 The uncertainty (2σ) of δ⁸²Se measurements, calculated from the twice the root mean square
 153 (RMS, 95% confidence level)³⁰ of 24 duplicate sample preparations and analysis, was 0.17‰.
 154 The value of the isotopic fractionation factor (α) was determined from the slope of the best-fit
 155 line from the linearized plot of ln(□⁸²Se + 1000‰) vs. ln(Se(VI))³¹. The uncertainties (2σ) of ε
 156 were ± 0.6‰, calculated from the scatter of the data points around the best-fit line using standard
 157 linear estimation methods.

158 Results and Discussion

159 **Se Concentrations in Rosita Groundwater and U Ore.** Se(VI) and Se(IV) concentrations in
 160 Rosita groundwater are provided in Table 1. Se(VI) is the dominant species with concentrations
 161 up to 306 μg/L in the groundwater samples while Se(IV) is found in fewer samples and only at
 162 concentrations below 9 μg/L. Generally, except for ore zone wells BL 3 and BL 4, groundwater

163 from the upgradient monitoring wells has higher Se(VI) compared to that in the ore zone or
164 downgradient monitoring wells. We did not observe any systematic pattern in the distribution of
165 Se(IV) at the site. Out of 12 samples with measurable Se(IV), 3 ore zone wells (BL 7, BL 29 and
166 BL 34) and one downgradient well, MW 37, contain only Se(IV) while the rest contain both
167 Se(VI) and Se(IV). In the previously mined parts of the site, the downgradient monitoring wells
168 MW 37, MW 75, MW 85, and MW 89, contain little (<1 µg/L) or no Se-oxyanions, either as
169 Se(VI) or Se(IV). The wells MW 32, MW 102, MW 103 and MW 137, located directly
170 downgradient of the mapped discontinuities of the ore body (Figure 2), contain substantial
171 amount of Se(VI) and in some cases Se(IV). In the unmined PAA 4, the downgradient wells
172 show little dissolved Se: MW 149 has no Se-oxyanions whereas MW 144 contains 0.6 µg/L
173 Se(VI) and Se(IV) below detection level (<0.1 µg/L).

174 The Se concentrations in the U ore collected at 7 discrete depths from borehole OZCH3
175 adjacent to the ore zone well BL 39 in the unmined PAA4 area, are low and vary from 24 µg/kg
176 to 48 µg/kg (Table 1). There is no apparent trend in the Se concentrations with depth. However,
177 the samples with the highest U concentrations collected from 70.71 – 71.32 m below the ground
178 surface also contain the highest amount of Se. The U ore was not characterized for the identity of
179 Se bearing minerals, but previous work identified ferroselite and elemental Se as the dominant
180 Se bearing species in South Texas and other roll-front type U deposits^{1,2,32-35}.

181 **Se Isotope Ratios in Rosita Groundwater and U Ore.** The $\delta^{82}\text{Se}$ in groundwater samples from
182 all PAAs and in the U ore are provided in Table 1. The $\delta^{82}\text{Se}$ of aqueous Se(VI) varies from
183 -1.46‰ to +6.14‰, with most of the samples showing elevated $\delta^{82}\text{Se}$ relative to the Se isotope
184 standard SRM 3149 (i.e., $\delta^{82}\text{Se} > 0.0\text{‰}$) (Figure 3). The highest $\delta^{82}\text{Se}$ of Se(VI) is observed in

185 groundwater from the ore zone well BL 39 from the unmined PAA4 area, while BL 3 from the
186 already mined PAA1 exhibits the most depleted $\delta^{82}\text{Se}$ value (-1.46‰). In a subset of samples
187 there is an apparent trend of increasing $\delta^{82}\text{Se}_{\text{VI}}$ with decreasing Se(VI) (Figure 3). Contrary to the
188 $\delta^{82}\text{Se}$ values of Se(VI), $\delta^{82}\text{Se}$ of Se(IV) is substantially depleted by up to -6.45‰ , except in
189 samples from BL 29 ($\delta^{82}\text{Se}_{\text{IV}} = 0.51\text{‰}$) and BL 34 ($\delta^{82}\text{Se}_{\text{IV}} = 0.73\text{‰}$). Notably, these wells had
190 no measurable Se(VI). In the samples containing both Se oxyanion species, Se(IV) is isotopically
191 lighter than Se(VI) with $\Delta^{82}\text{Se}$ ($\approx \delta^{82}\text{Se}_{\text{VI}} - \delta^{82}\text{Se}_{\text{IV}}$) ranging from 3.5‰ to 6.9‰ . We observe a
192 weak correlation between Se(IV) concentration and $\delta^{82}\text{Se}_{\text{IV}}$ of the groundwater samples; the
193 $\delta^{82}\text{Se}_{\text{IV}}$ decreases with decreasing Se(IV) (Figure S1).

194 The Se isotope compositions of the Se minerals in the U ore from 7 discrete depths are
195 provided in Table 1. The $\delta^{82}\text{Se}$ of the U ore ranges from -1.28‰ to -0.40‰ . The median value
196 of -0.72‰ is low relative to the majority of the groundwater Se(VI) samples (Figure 3). There is
197 also an enrichment in $\delta^{82}\text{Se}$ in the ore with increasing depth.

198 **Implication of Se Isotopic Signature of Rosita U ore.** Our observations of ^{82}Se depletion of
199 the ore are limited to a single borehole (OZCH3) in PAA4, which does not provide the full extent
200 of the spatial variability in $\delta^{82}\text{Se}$ of the ore body. Furthermore, the U ore samples from the
201 borehole OZCH3 are not representative of the Se-enriched portion of the roll-front system
202 generated by reductive precipitation of Se. Lower Se concentrations of the U ore compared to
203 that of upgradient groundwater suggest a Se rich sediment upgradient of the borehole OZCH3
204 (Table 1, Figure 3). This is further supported by our observation of ^{82}Se depletion in the U ore.
205 Ideally, reductive precipitation of Se-oxyanions at the redox interface should produce ^{82}Se
206 depleted Se minerals at the upgradient fringe of the roll-front deposit. With increasing distance

207 along the hydraulic gradient, the Se minerals should become isotopically heavier. However, after
208 complete removal of Se-oxyanions from the groundwater, the Se concentrations and isotopic
209 composition of the sediments should return to background values. The sediments collected 6m
210 above the ore-bearing zone contain 24.3 µg/kg of Se with a $\delta^{82}\text{Se}$ of -1.54% , resembling the ore-
211 zone sediments both in terms of Se concentrations and isotopic composition (Table 1).
212 Therefore, we surmise that Se concentrations and isotopic compositions of our U ore samples
213 reflect the primary Se content of the aquifer sediments.

214 **Se Reduction in Groundwater: Se Concentration Distribution and Geochemical**
215 **Conditions.** The distribution of dissolved Se in Rosita groundwater is consistent with reduction
216 of Se oxyanions, particularly Se(VI) reduction, by naturally occurring reducing environments
217 within and downgradient of the ore zone. The Se(VI) hotspots at the upgradient wells or ore zone
218 wells in the mined part of the site resulted from the oxidation of Se minerals either during mining
219 or by interaction with the oxygenated recharge water. For example, high Se(VI) up to 107 µg/L
220 in the upgradient wells MW 158 and MW 154 in the unmined PAA 4 is likely to reflect natural
221 dissolution of Se minerals in the aquifer. In absence of any Se removal within or downgradient
222 of the ore zone, the downgradient wells should show Se(VI) concentrations similar to that of the
223 upgradient wells. Little or no Se oxyanions in the downgradient wells, particularly in MW 37,
224 MW 75, MW 85, and MW 89, suggests Se removal before groundwater arrives at these wells. At
225 the study site, a progression from nitrate-reducing, to Fe(III)-reducing, and then to U(VI)-
226 reducing conditions along the hydraulic gradient is inferred from concentrations of the redox
227 species (e.g., NO_3^- , Fe(II) and U(VI)), Eh values and isotopic measurements (e.g., $\delta^{15}\text{N}$, and
228 $\delta^{238}\text{U}$) of groundwater samples¹⁷. Among the downgradient wells investigated by Basu et al.

229(2015), the samples from MW 37, MW 75, MW 85, and MW 89 exhibited low Eh (-11.7 mV to
230-105.5 mV), low U(VI) concentrations (< 20 µg/L) and highly depleted $\delta^{238}\text{U}$ (-1.41‰ to
231-2.49‰) suggesting naturally occurring reducing environments capable of U(VI) and thus,
232Se(VI) reduction. The overall range of Eh and pH suggests thermodynamic favorability of Se-
233oxyanions reduction in Rosita groundwater (Figure 1). The decrease in Se(VI) along the
234hydraulic gradient is therefore consistent with the Se(VI) and perhaps Se(IV) reduction in
235downgradient the reducing environments suggested by Basu et al. 2015 based on U isotopes and
236other evidence. Alternatively, Se(IV) could be strongly adsorbing and removed via sorption onto
237minerals.

238 Several downgradient wells, however, do not follow the general trend of aqueous Se(VI)
239removal along the hydraulic gradient. These wells, MW 32, MW 102, MW 103, and MW 137,
240are located directly downgradient of the mapped gaps in the ore body (Figure 2). These gaps may
241mark regions that lacked the reducing materials that were responsible for the formation of the ore
242body in the adjacent areas. This difference implies an unrestricted flow of the upgradient water
243rich in Se(VI) and other oxidants (e.g., NO_3^-) (Figure S2) and with a high Eh to the downgradient
244wells MW 32, MW 102, MW 103, and MW 137 through these gaps, which is consistent with the
245observations reported in ref 18. The postmining restoration fluid with high residual Se(VI) is
246unlikely to arrive at the downgradient wells due to low groundwater velocity (3-6 m/year) and
247restriction of flow by net withdrawal of groundwater during restoration. However, the presence
248of the reduction product Se(IV) in MW 32 and MW 103 suggest existing Se(VI) reducing
249conditions in these wells which is also supported by our Se isotope data (see below).

250 **Se Reduction in Groundwater: Se Isotope Ratios.** If all of the variation of $\delta^{82}\text{Se}$ were due to
251 reduction of Se from a single Se source by a single mechanism, a strong correlation between
252 $\delta^{82}\text{Se}$ and concentrations of Se-oxyanions would be expected. We did not observe a strong
253 correlation between $\delta^{82}\text{Se}$ and Se(VI) concentrations which suggests heterogeneous Se sources
254 and complex Se cycling mechanisms. However, the samples that exhibit highly enriched $\delta^{82}\text{Se}$ (>
255 4‰) can only be generated by reduction of Se(VI). In the following paragraphs, we discuss the
256 evidence of Se(VI) reduction from the $\delta^{82}\text{Se}$ data from Rosita groundwater along with potential
257 alternative mechanisms with their limitations.

258 In addition to the distribution of Se-oxyanion concentrations, Se isotope data from Rosita U
259 ore and groundwater samples help identify pathways of Se-cycling and delineate Se(VI) reducing
260 zones at the study site. The upgradient groundwater currently entering the roll-front system is
261 Se(VI)-rich with concentrations ranging from 32 $\mu\text{g/L}$ to 137 $\mu\text{g/L}$ (median Se(VI) = 94.84
262 $\mu\text{g/L}$). The $\delta^{82}\text{Se}$ of the upgradient groundwater also varies from -1.12‰ to $+2.22\text{‰}$, with an
263 average $\delta^{82}\text{Se}$ of 0.51‰ . Since the roll-front system reduces and captures all incoming Se(VI),
264 we hypothesize that the average $\delta^{82}\text{Se}$ of the U ore should be identical to the average $\delta^{82}\text{Se}$ of
265 incoming groundwater, assuming that the Se inputs for the U ore were similar to that observed in
266 the present system.

267 If dissolution of Se minerals were the only mechanism responsible for the observed
268 distribution of Se(VI) in Rosita groundwater, we would expect the groundwater samples to be
269 similar to the inferred average $\delta^{82}\text{Se}$ of the U ore ($\sim 0.5\text{‰}$). The oxidative dissolution of U ore
270 should yield aqueous Se(VI) with similar isotopic composition as quantitative layer-by-layer
271 dissolution of Se mineral grains results in negligible isotopic fractionation. However, it is

272 possible for the postmining groundwater to acquire Se with a range of $\delta^{82}\text{Se}$ values (e.g., -1.5‰
273 to $\sim 2\text{‰}$), because we expect the isotopic composition of Se minerals to exhibit spatial variability
274 in the ore zone. Aqueous Se isotope compositions outside the -1.5‰ to 2.0‰ range suggest an
275 alternate or additional process affecting the Se isotope composition of the groundwater. -

276 The enrichments in $\delta^{82}\text{Se}$ of Rosita groundwater relative to the inferred average $\delta^{82}\text{Se}$ of the U
277 ore are likely caused by Se(VI) reduction in Rosita groundwater. With ongoing reduction of
278 Se(VI), the unreacted remaining Se(VI) exhibits ^{82}Se enrichment^{20-26,29}, while the intermediate
279 product Se(IV) is first enriched in the lighter isotopes (i.e., ^{76}Se), and later upon further reduction
280 to Se(0) and possibly complete removal of Se(VI), is enriched in ^{82}Se . The largest $^{82}\text{Se}_{\text{VI}}$
281 enrichments observed in the ore zone wells BL 17 and BL 39 are 5.19‰ and 6.14‰ ,
282 respectively, suggesting a maximum offset of $\sim 6\text{‰}$ from that of the inferred $\delta^{82}\text{Se}$ of the U ore.
283 In all samples containing both Se(VI) and Se(IV), Se(IV) is isotopically lighter (i.e. enriched in
284 ^{76}Se , $-6.38\text{‰} < \delta^{82}\text{Se} < 0\text{‰}$). This suggests that Se(IV) is a product of Se(VI) reduction rather than
285 arising from the oxidation of the U ore. In addition, the two groundwater samples with $^{82}\text{Se}_{\text{IV}}$
286 enrichment (i.e., $\delta^{82}\text{Se}_{\text{IV}} > 0\text{‰}$) have low Eh ($\text{Eh}_{\text{BL } 29} = -82.5 \text{ mV}$ and $\text{Eh}_{\text{BL } 34} = -59.4 \text{ mV}$) and
287 no detectable Se(VI). This ^{82}Se enrichment in Se(IV) and a lack of Se(VI) suggests extensive
288 reduction of Se(IV) has occurred in the absence of production of Se(IV) via Se(VI) reduction.

289 The correlation between Se isotopic shifts and changes in Se oxyanion concentrations also
290 suggests aqueous Se(VI) reduction. When Se(VI) data from all wells are pooled together, we
291 observe two distinct trends in the relationship between $\delta^{82}\text{Se}$ values and Se(VI) concentrations
292 (Figure 2). First, there is an increasing trend in $\delta^{82}\text{Se}$ with decreasing Se(VI). Second, for several
293 wells such as BL 8, BL 10, MW 102, MW 103, MW 53, and MW 137, Se(VI) concentrations

294 decrease with no major shift in the $\delta^{82}\text{Se}$. In samples showing no major change in $\delta^{82}\text{Se}$,
295 particularly in BL 8, BL 10, MW 102, and MW 103, the decrease in Se(VI) may be attributed to
296 a localized mixing with groundwater with relatively low Se, similar to that of MW 42, which is
297 also consistent with relatively high Eh values and NO_3^- concentrations (Figure S2) in these
298 wells¹⁷. Alternatively, a more likely scenario is that these samples may have acquired variable
299 amounts of Se from the Se-rich zone in the roll-front with a $\delta^{82}\text{Se}$ similar to the inferred average
300 $\delta^{82}\text{Se}$ of the roll-front. The first trend where $\delta^{82}\text{Se}$ in a subset of samples increased with
301 decreasing Se(VI) conforms to a Rayleigh-type fractionation model with $\epsilon = -2.25\text{‰} \pm 0.61\text{‰}$
302 calculated excluding Se data from the wells containing measurable NO_3^- . This strongly suggest
303 Se(VI) reduction as the primary mechanism of Se(VI) concentration decrease in these samples.

304 Two alternative mechanisms, mixing and equilibrium isotopic exchange, with the potential to
305 influence the Se isotopic signature of Rosita groundwater are unlikely to play any major role at
306 the study site. The elevation in $\delta^{82}\text{Se}$ of Se(VI) in BL 39 and BL 17 above $\sim 2\text{‰}$ cannot be
307 generated by mixing ore-zone groundwater with an average $\delta^{82}\text{Se}$ of 0.5‰ with the upgradient
308 water entering the system with a maximum $\delta^{82}\text{Se}$ of $\sim 2\text{‰}$. Therefore, mixing cannot account for
309 the observed elevated $\delta^{82}\text{Se}$ values of Se(VI) in BL 39 and BL 17. Also, an equilibrium isotopic
310 exchange between coexisting dissolved species Se(VI) and Se(IV) or more reduced Se species
311 would lead to ^{82}Se enrichment in Se(VI). This seems highly unlikely under the prevalent
312 geochemical conditions that are far from chemical equilibrium. The rates of exchange between
313 Se(VI) and Se(IV), which requires transfer of two electrons, have yet to be determined.
314 However, based on recent reports on U(VI)-U(IV) exchange also requiring two electrons
315 transferred³⁶, very slow exchange (100 to 1000 yrs) between Se(VI) and Se(IV) may be inferred

316at very low concentrations (i.e. < 9 µg/L) of Se(IV). In addition, Se(VI)-Se(IV) exchange may
317further be inhibited by removal of Se(IV) by either adsorption or by reduction to Se(0)^{20,37}.

318 **Se Isotopes as Redox Indicators in the Unmined Area.** In addition to serving as an indicator
319for reduction of potentially toxic Se-oxyanions in groundwater, Se isotope ratios may also
320provide useful information in the context of U(VI) reduction at ISR sites. The results from the
321unmined PAA 4 area demonstrate that stable Se isotope ratios are effective indicators of the
322areas approaching U(VI) reducing conditions (Table S1). Our previous work on U isotope ratios
323(²³⁸U/²³⁵U, expressed as $\delta^{238}\text{U}$)¹⁷ showed evidence of U(VI) reduction in the transect containing
324MW 158, BL 36, and MW 144 along the hydraulic gradient, particularly in the ore zone BL and
325the downgradient well, while there was a lack of U(VI) reducing conditions along another
326transect (MW 154, BL 39, MW 149) (Figure 2, Table S1). Along both transects, a decrease in
327NO₃⁻ in groundwater from ≥12 mg/L in the upgradient wells to below detection in the ore zone
328BL wells and downgradient wells was also reported¹⁷. The western transect, where the lack of a
329large ²³⁸U depletion in groundwater indicated the absence of U(VI) reduction in the ore zone well
330BL 39 ($\delta^{238}\text{U} = 0.56\text{‰}$) and downgradient MW 149 ($\delta^{238}\text{U} = 0.48\text{‰}$), shows an overall
331enrichment in $\delta^{82}\text{Se}$ of Se(VI) up to ~6‰ relative to the average $\delta^{82}\text{Se}$ (0.5‰) of the U ore with
332BL 39 exhibiting a $\delta^{82}\text{Se}$ of 6.14‰. This $\delta^{82}\text{Se}$ of Se(VI) in BL 39 is ~4‰ higher compared to
333that of the upgradient well MW 154 ($\delta^{82}\text{Se} = 2.19\text{‰}$). Se(VI) in the downgradient well MW 149
334is below the detection limit (< 0.1 µg/L). This suggests progressively stronger Se(VI) reducing
335conditions along the hydraulic gradient.

336 In comparison, the upgradient well MW 158 ($\delta^{238}\text{U} = -0.08\text{‰}$) from the western transect
337shows ⁸²Se depletion ($\delta^{82}\text{Se}_{\text{VI}} = -1.12\text{‰}$) with a lower Se(VI) concentration suggesting spatial

338 heterogeneity both in terms of background Se content and isotopic composition. However, the
339 wells along the hydraulic gradient in this transect with highly fractionated U isotope ratios, BL
34036 ($\delta^{238}\text{U} = -1.61\text{‰}$) and MW 144 ($\delta^{238}\text{U} = -1.96\text{‰}$) have very little or no detectable Se
341 oxyanions suggesting either almost quantitative reduction of Se(VI) and Se(IV) and/or removal
342 of Se(IV) via adsorption onto aquifer material. Thus the results from the unmined PAA4
343 demonstrate the effectiveness of Se isotope ratios in delineating Se(VI) reducing environments
344 and in providing additional information about existing redox conditions that can not be obtained
345 from the U isotopic data alone.

346 **Fractionation Mechanisms at Rosita and Comparison of ϵ with Previous Studies.** The
347 magnitude of the Se isotope fractionation observed at Rosita is more consistent with a microbial
348 reduction mechanism than with abiotic reduction, but there is still sufficient uncertainty that
349 abiotic reduction cannot be ruled out. Johnson et al. 2011 provides a detailed review of the
350 magnitudes of Se isotope fractionation for various abiotic reductants and microbial species.
351 Microbial reduction of Se-oxyanions yields a range of ϵ values, spanning from -0.3‰ to -7.5‰
352 for the reduction of Se(VI) to Se(IV) and from -1.7‰ to -12‰ for the reduction of Se(IV) to
353 Se(0). The abiotic reduction of Se generally yields consistently large ($> -10\text{‰}$) isotopic
354 fractionations. The ϵ for reduction of Se(VI) to Se(IV) by the Fe(II)-Fe(III) layered double
355 hydroxide mineral “green rust”, a likely reductant in soils and sediments, is $\sim -11\text{‰}$ while the
356 reduction of Se(IV) to Se(0) by FeS and NH_2OH or ascorbic acid produces a fractionation (as ϵ)
357 of -10‰ , and -15.0 to -19.2‰ , respectively. The ϵ determined from the groundwater samples
358 from the Rosita ISR site ($-2.25\text{‰} \pm 0.61\text{‰}$) is much smaller compared to that observed during
359 abiotic Se(VI) reduction and falls within the range observed during Se(VI) reduction by natural
360 microbial consortia²³. Despite some heterogeneities, the observed sequence of redox reactions

361 along the hydraulic gradient from NO_3^- reducing to Fe(III)- and U(VI)-reducing environments is
362 also consistent with the microbially mediated redox ladder in aquifers³⁸. However, reservoir
363 effects arising from the lack of chemical communication between the zones of reduction (e.g.,
364 biofilms, or mineral surfaces in clay-rich zones) and the bulk dissolved Se(VI) in the more
365 rapidly flowing parts of the sandy aquifer may limit the expression of overall isotopic
366 fractionation in groundwater samples and thus lead to a diminished apparent ϵ value²⁹. Future
367 research involving similar sites should be directed toward identification of the Se reduction
368 mechanism and determination of ϵ at the site using analysis of the temporal trend of Se-oxyanion
369 concentrations with Se isotope ratios from the target wells as complemented by laboratory
370 experiments for the site-specific reduction mechanism.

371 **Implications for Detection and Monitoring of Se and U Reduction at ISR sites.** The results
372 of this study demonstrate that Se isotope ratios are effective indicators of natural attenuation of
373 Se(VI), a residual product of ISR mining and a potential water contaminant for several ISR sites.
374 Due to similarities in the redox potentials for U(VI) and Se(VI) reduction, the $\delta^{82}\text{Se}$ values in
375 groundwater can also indicate whether the present redox state is approaching U(VI) reducing
376 conditions. Furthermore, our results suggest that the Se isotope ratios record the redox
377 environments precursory to U(VI) reducing conditions that cannot be obtained from the
378 concentration (e.g., Se(VI) or U(VI)) data alone.

379 Se isotope ratios may be more effective in detecting conditions conducive for remediation of
380 U(VI) than the U isotope ratios of groundwater samples. A recent investigation suggests that in
381 contrast to microbial reduction, abiotic reduction of U(VI) does not significantly fractionate U
382 isotopes³⁹. Aqueous and adsorbed Fe(II)^{40,41}, magnetite^{42,43} and titanomagnetite⁴⁴, and FeS^{45,46}
383 (both residual after mining and biogenic) may readily reduce U(VI) in aquifers. These abiotic

384reductants are also capable of reducing Se(IV)⁴⁷⁻⁵⁰. In that case, compared to $\delta^{238}\text{U}$, $\delta^{82}\text{Se}$ of
385groundwater would be a more reliable indicator of conditions approaching U(VI) reduction, and
386an improved characterization of the existing redox state and reducing capacity of the aquifer,
387which is required to demonstrate potential for natural U(VI) reduction. In aquifers with a need
388for active remediation, the knowledge of the existing redox state is also important to determine
389the remediation strategy and the choice of reductant (if used) to avoid aggressive reductive
390remediation, which may mobilize contaminants such as arsenic. Furthermore, Se(VI) reduction
391in the absence of any significant U(VI) reduction could also imply slower kinetics for U(VI)
392reduction.

393 Our measurements on Se speciation and stable Se isotopes reveal the spatial distribution at a
394single time and do not provide direct information on time-dependent changes in Se oxyanion
395concentrations and concomitant changes in Se isotope ratios. Efficient post-mining monitoring of
396reduction would include time series measurements of Se oxyanion concentration and Se isotope
397ratios in samples from the target ore zone BL wells or wells from the monitoring ring. This
398would enable more accurate determination of the exact relationship between the changes in
399Se(VI) and/or Se(IV) concentrations in a target well and the associated shifts in $\delta^{82}\text{Se}$ (or the site-
400specific isotopic fractionation factor), which is required for the quantification of Se(VI)
401remediation.

402 **Acknowledgements.** This research was funded by the UC Laboratory Fees Research Program.
403We thank Uranium Resources, Inc. for providing site access and logistic support during sample
404collection and drilling.

405 **Associated Content.** Correlation between $\delta^{82}\text{Se}_{\text{IV}}$ and Se(IV), and distribution of NO_3^- in
406Rosita groundwater Comparison between Se(VI) and U(VI) concentrations in groundwater from
407PAA 4 along with Se ($\delta^{82}\text{Se}$) and U isotope ratios ($\delta^{238}\text{U}$), are provided in the Supporting
408Information. This information is available free of charge via the Internet at <http://pubs.acs.org>.

409References

- 410(1) Howard, J. H. Geochemistry of selenium: formation of ferroselite and selenium behavior
411 in the vicinity of oxidizing sulfide and uranium deposits. *Geochimica et Cosmochimica*
412 *Acta* **1977**, *41* (11), 1665–1678.
- 413(2) Dahlkamp, F. J. *Uranium deposits of the world*; 2009.
- 414(3) Granger, H. C.; Warren, C. G. Unstable sulfur compounds and the origin of roll-type
415 uranium deposits. *Economic Geology* **1969**, *64* (2), 160–171.
- 416(4) Xiong, Y. Predicted equilibrium constants for solid and aqueous selenium species to 300
417 °C: applications to selenium-rich mineral deposits. *Ore Geology Reviews* **2003**, *23* (3-4),
418 259–276.
- 419(5) Beath, O. A.; Hagner, A. F.; Gilbert, C. S. *Some rocks and soils of high selenium*
420 *content*; University of Wyoming, 1946; Vol. 36.
- 421(6) Dribus, J. R.; Nanna, R. F. *National uranium resource evaluation, Rawlins quadrangle,*
422 *Wyoming and Colorado*; Bendix Field Engineering Corp., Grand Junction, CO (USA),
423 1982.
- 424(7) Plant, J. A.; Bone, J.; Voulvoulis, N.; Kinniburgh, D. G. Arsenic and selenium. **2014**.
- 425(8) Bartz, G. L. Uranium prospecting based on selenium and molybdenum. **1982**.
- 426(9) Muscatello, J. R.; Belknap, A. M.; Janz, D. M. Accumulation of selenium in aquatic
427 systems downstream of a uranium mining operation in northern Saskatchewan, Canada.
428 *Environmental Pollution* **2008**, *156* (2), 387–393.
- 429(10) Muscatello, J. R.; Bennett, P. M.; Himbeault, K. T.; Belknap, A. M.; Janz, D. M. Larval
430 Deformities Associated with Selenium Accumulation in Northern Pike (*Esox lucius*)
431 Exposed to Metal Mining Effluent. *Environ. Sci. Technol.* **2006**, *40* (20), 6506–6512.
- 432(11) van METRE, P. C.; GRAY, J. R. Effects of uranium mining discharges on water quality
433 in the Puerco River basin, Arizona and New Mexico. *Hydrological Sciences Journal*
434 **1992**, *37* (5), 463–480.
- 435(12) Williams, K. H.; Wilkins, M. J.; N'Guessan, A. L.; Arey, B.; Dodova, E.; Dohnalkova,
436 A.; Holmes, D.; Lovley, D. R.; Long, P. E. Field evidence of selenium bioreduction in a
437 uranium-contaminated aquifer. **2013**, *5* (3), 444–452.
- 438(13) OECD, I. *Uranium 2011: Resources*; Production, 2012.
- 439(14) Vance, R. Uranium 2014: Resources, Production and Demand. **2014**.
- 440(15) Ramirez, P., Jr; Rogers, B. P. Selenium in a Wyoming Grassland Community Receiving
441 Wastewater from an In Situ Uranium Mine. *Archives of Environmental Contamination*
442 *and Toxicology* **2002**, *42* (4), 431–436.
- 443(16) Davis, J. A.; Curtis, G. P. *Consideration of geochemical issues in groundwater*
444 *restoration at uranium in-situ leach mining facilities (NUREG/CR-6870)*; USGS, 2007.
- 445(17) Basu, A.; Brown, S. T.; Christensen, J. N.; DePaolo, D. J.; Reimus, P. W.; Heikoop, J.
446 M.; Woldegabriel, G.; Simmons, A. M.; House, B. M.; Hartmann, M.; et al. Isotopic and
447 Geochemical Tracers for U(VI) Reduction and U Mobility at an in Situ Recovery U
448 Mine. *Environ. Sci. Technol.* **2015**, *49* (10), 5939–5947.
- 449(18) Maher, K.; Bargar, J. R.; Brown, G. E., Jr. Environmental Speciation of Actinides.
450 *Inorg. Chem.* **2013**, *52* (7), 3510–3532.

- 451(19) Seby, F.; Potin-Gautier, M.; Giffaut, E.; Borge, G. A critical review of thermodynamic
452 data for selenium species at 25 C. *Chemical ...* **2001**, 171 (3-4), 173–194.
- 453(20) Johnson, T. M. Stable Isotopes of Cr and Se as Tracers of Redox Processes in Earth
454 Surface Environments. In *Advances in Isotope Geochemistry*; Springer Berlin
455 Heidelberg: Berlin, Heidelberg, 2011; pp 155–175.
- 456(21) Johnson, T. M.; Bullen, T. D. Mass-Dependent Fractionation of Selenium and
457 Chromium Isotopes in Low-Temperature Environments. *Reviews in mineralogy and ...*
458 **2004**.
- 459(22) Johnson, T. M.; Bullen, T. D. Selenium isotope fractionation during reduction by Fe (II)-
460 Fe (III) hydroxide-sulfate (green rust). *Geochimica et Cosmochimica Acta* **2003**, 67 (3),
461 413–419.
- 462(23) Ellis, A. S.; Johnson, T. M.; Herbel, M. J.; Bullen, T. D. ScienceDirect.com - Chemical
463 Geology - Stable isotope fractionation of selenium by natural microbial consortia.
464 *Chemical Geology* **2003**.
- 465(24) Herbel, M. J.; Johnson, T. M.; Oremland, R. S.; Bullen, T. D. Fractionation of selenium
466 isotopes during bacterial respiratory reduction of selenium oxyanions. *Geochimica et*
467 *Cosmochimica Acta* **2000**, 64 (21), 3701–3709.
- 468(25) Mitchell, K.; Couture, R.-M.; Johnson, T. M.; Mason, P. R. D.; Van Cappellen, P.
469 Selenium sorption and isotope fractionation: Iron(III) oxides versus iron(II) sulfides.
470 *Chemical Geology* **2013**, 342 (C), 21–28.
- 471(26) Johnson, T. M.; Herbel, M. J.; Bullen, T. D.; Zawislanski, P. T. Selenium isotope ratios
472 as indicators of selenium sources and oxyanion reduction. *Geochimica et Cosmochimica*
473 *Acta* **1999**, 63 (18), 2775–2783.
- 474(27) Schilling, K.; Johnson, T. M.; Mason, P. R. D. A sequential extraction technique for
475 mass-balanced stable selenium isotope analysis of soil samples. *Chemical Geology* **2014**,
476 381 (C), 125–130.
- 477(28) Schilling, K.; Johnson, T. M.; Dhillon, K. S.; Mason, P. R. D. Fate of selenium in soils
478 at a seleniferous site recorded by high precision Se isotope measurements. *Environ. Sci.*
479 *Technol.* **2015**, 150715110835008–150715110835009.
- 480(29) Clark, S. K.; Johnson, T. M. Effective Isotopic Fractionation Factors for Solute Removal
481 by Reactive Sediments: A Laboratory Microcosm and Slurry Study. *Environ. Sci.*
482 *Technol.* **2008**, 42 (21), 7850–7855.
- 483(30) Hyslop, N. P.; White, W. H. Estimating Precision Using Duplicate Measurements.
484 *Journal of the Air & Waste Management Association* **2009**, 59 (9), 1032–1039.
- 485(31) Scott, K. M.; Lu, X.; Cavanaugh, C. M.; Liu, J. S. Optimal methods for estimating
486 kinetic isotope effects from different forms of the Rayleigh distillation equation.
487 *Geochimica et Cosmochimica Acta* **2004**, 68 (3), 433–442.
- 488(32) Reynolds, R. L.; Goldhaber, M. B. Iron disulfide minerals and the genesis of roll-type
489 uranium deposits. *Economic Geology* **1983**, 78 (1), 105–120.
- 490(33) REYNOLDS, R. L.; GOLDHABER, M. B. Origin of a South Texas Roll-Type Uranium
491 Deposit .1. Alteration of Iron-Titanium Oxide Minerals. *Economic Geology* **1978**, 73
492 (8), 1677–1689.
- 493(34) Huang, W. H. Geochemical and sedimentologic problems of uranium deposits of Texas

- 494 Gulf Coastal Plain. *AAPG Bulletin* **1978**.
- 495(35) Granger, H. C. Ferroselite in a roll-type uranium deposit, Powder River Basin,
496 Wyoming. *US Geological Survey Professional Paper* **1966**, C133–C137.
- 497(36) Wang, X.; Johnson, T. M.; Lundstrom, C. C. Low temperature equilibrium isotope
498 fractionation and isotope exchange kinetics between U(IV) and U(VI). *Geochimica et*
499 *Cosmochimica Acta* **2015**, 1–14.
- 500(37) White, A. F.; Benson, S. M.; Yee, A. W.; Wollenberg, H. A.; Flexser, S. Groundwater
501 contamination at the Kesterson Reservoir, California: 2. Geochemical parameters
502 influencing selenium mobility. *Water Resour. Res.* **1991**, 27 (6), 1085–1098.
- 503(38) McMahon, P. B.; Chapelle, F. H. Redox Processes and Water Quality of Selected
504 Principal Aquifer Systems. *Ground Water* **2008**, 46 (2), 259–271.
- 505(39) Stylo, M.; Neubert, N.; Wang, Y.; Monga, N.; Romaniello, S. J.; Weyer, S.; Bernier-
506 Latmani, R. Uranium isotopes fingerprint biotic reduction. *Proc. Natl. Acad. Sci. U.S.A.*
507 **2015**, 201421841–201421846.
- 508(40) Du, X.; Boonchayaanant, B.; Wu, W.-M.; Fendorf, S.; Bargar, J.; Criddle, C. S.
509 Reduction of Uranium(VI) by Soluble Iron(II) Conforms with Thermodynamic
510 Predictions. *Environ. Sci. Technol.* **2011**, 45 (11), 4718–4725.
- 511(41) Taylor, S. D.; Marcano, M. C.; Rosso, K. M.; Becker, U. An experimental and ab initio
512 study on the abiotic reduction of uranyl by ferrous iron. *Geochimica et Cosmochimica*
513 *Acta* **2015**, 156 (C), 154–172.
- 514(42) Latta, D. E.; Gorski, C. A.; Boyanov, M. I.; O’Loughlin, E. J.; Kemner, K. M.; Scherer,
515 M. M. Influence of Magnetite Stoichiometry on U VI Reduction. *Environ. Sci. Technol.*
516 **2012**, 46 (2), 778–786.
- 517(43) Yuan, K.; Renock, D.; Ewing, R. C.; Becker, U. Uranium reduction on magnetite:
518 Probing for pentavalent uranium using electrochemical methods. *Geochimica et*
519 *Cosmochimica Acta* **2015**, 156 (C), 194–206.
- 520(44) Latta, D. E.; Pearce, C. I.; Rosso, K. M.; Kemner, K. M.; Boyanov, M. I. Reaction of U
521 VI with Titanium-Substituted Magnetite: Influence of Ti on U IV Speciation. **2013**, 47
522 (9), 4121–4130.
- 523(45) Veeramani, H.; Scheinost, A. C.; Monsegue, N.; Qafoku, N. P.; Kukkadapu, R.;
524 Newville, M.; Lanzirrotti, A.; Pruden, A.; Murayama, M.; Hochella, M. F., Jr. Abiotic
525 Reductive Immobilization of U(VI) by Biogenic Mackinawite. *Environ. Sci. Technol.*
526 **2013**, 47 (5), 2361–2369.
- 527(46) Troyer, L. D.; Tang, Y.; Borch, T. Simultaneous Reduction of Arsenic(V) and
528 Uranium(VI) by Mackinawite: Role of Uranyl Arsenate Precipitate Formation. *Environ.*
529 *Sci. Technol.* **2014**, 141124120622003.
- 530(47) Myneni, S.; Tokunaga, T. K.; Brown, G. E. Abiotic selenium redox transformations in
531 the presence of Fe(II,III) oxides. *Science* **1997**, 278 (5340), 1106–1109.
- 532(48) Scheinost, A. C.; Charlet, L. Selenite Reduction by Mackinawite, Magnetite and
533 Siderite: XAS Characterization of Nanosized Redox Products. *Environ. Sci. Technol.*
534 **2008**, 42 (6), 1984–1989.
- 535(49) Charlet, L.; Scheinost, A. C.; Tournassat, C.; Greneche, J. M.; Géhin, A.; Fernández-
536 Martı nez, A.; Coudert, S.; Tisserand, D.; Brendle, J. Electron transfer at the

537 mineral/water interface: Selenium reduction by ferrous iron sorbed on clay. *Geochimica*
538 *et Cosmochimica Acta* **2007**, 71 (23), 5731–5749.
539(50) Baik, M. H.; Lee, S. Y.; Jeong, J. Sorption and reduction of selenite on chlorite surfaces
540 in the presence of Fe(II) ions. *Journal of Environmental Radioactivity* **2013**, 126 (c),
541 209–215.
542
543

544Table 1. Se concentrations and isotope ratios in Rosita groundwater and U ore.

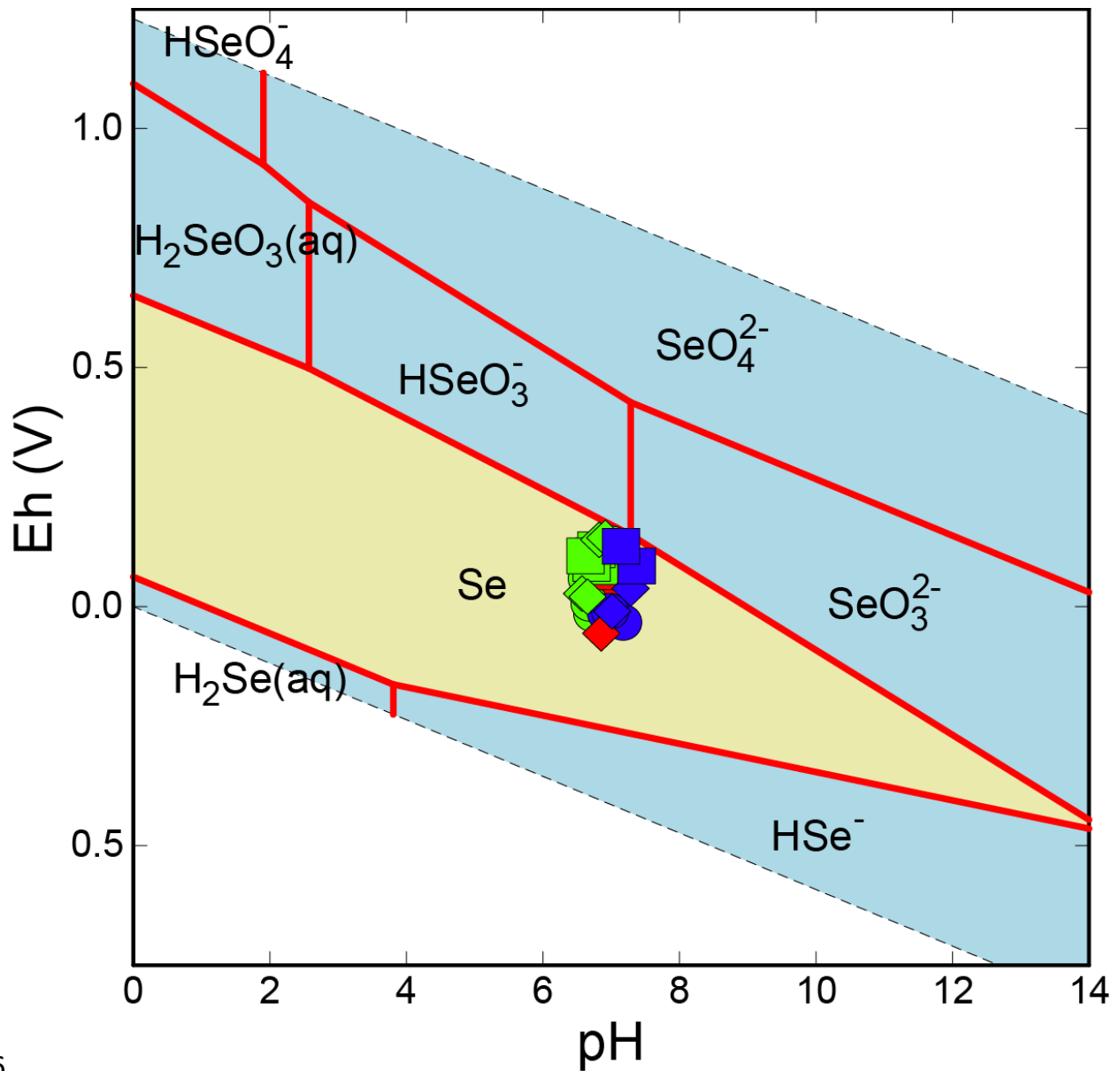
Rosita Groundwater						
Well	Location	PAA	Se(VI) ppb	$\delta^{82}\text{Se}_{\text{VI}}$	Se(IV) ppb	$\delta^{82}\text{Se}_{\text{IV}}$
BL 3	Ore zone	1	306.06	-1.46‰	<0.1	
BL 4	Ore zone	1	44.02	0.97‰	<0.1	
BL 7	Ore zone	1	<0.1		8.78	-1.36‰
BL 8	Ore zone	1	6.08	0.82‰	<0.1	
BL 9	Ore zone	2	<0.1		<0.1	
BL 10	Ore zone	2	9.32	0.97‰	<0.1	
BL 17	Ore zone	2	12.51	5.19‰	<0.1	
BL 22	Ore zone	2	<0.1		<0.1	
BL 28	Ore zone	3	<0.1		<0.1	
BL 29	Ore zone	3	<0.1		3.18	0.51‰
BL 34	Ore zone	3	<0.1		8.22	0.73‰
MW 25	Upgradient	1	59.87	0.58‰	8.17	-2.92‰
MW 26	Upgradient	1	112.27	0.9‰	0.4	ND
MW 32	Downgradient	1	66.56	0.45‰	1.29	-6.45‰
MW 37	Downgradient	1	<0.1		0.15	-2.63‰
MW 42	Upgradient	2	<0.1		<0.1	
MW 45	Upgradient	2	106.62	-0.47‰	0.61	ND
MW 53	Upgradient	2	31.59	0.83‰	0.24	ND
MW 66	Upgradient	2	63.87	0.7‰	<0.1	
MW 75	Downgradient	3	<0.1		<0.1	
MW 85	Downgradient	2	<0.1		<0.1	
MW 89	Downgradient	2	<0.1		<0.1	
MW 102	Downgradient	2	10.38	1.12‰	<0.1	

MW 103	Downgradient	2	6.26	0.59‰	0.2	-4.66‰
MW 129	Upgradient	3	137.01	0.43‰	4.35	-3.69‰
MW 131	Upgradient	3	94.84	0.54‰	<0.1	
MW 137	Downgradient	3	29.72	0.51‰	<0.1	
BL 36	Ore zone	4	<0.1		<0.1	
BL 39	Ore zone	4	8.97	6.14‰	2.87	-0.61‰
MW144	Downgradient	4	0.6	ND	<0.1	
MW149	Downgradient	4	<0.1		<0.1	
MW154	Upgradient	4	107.44	2.22‰	<0.1	
MW158	Upgradient	4	48.83	-1.12‰	<0.1	

Rosita U ore

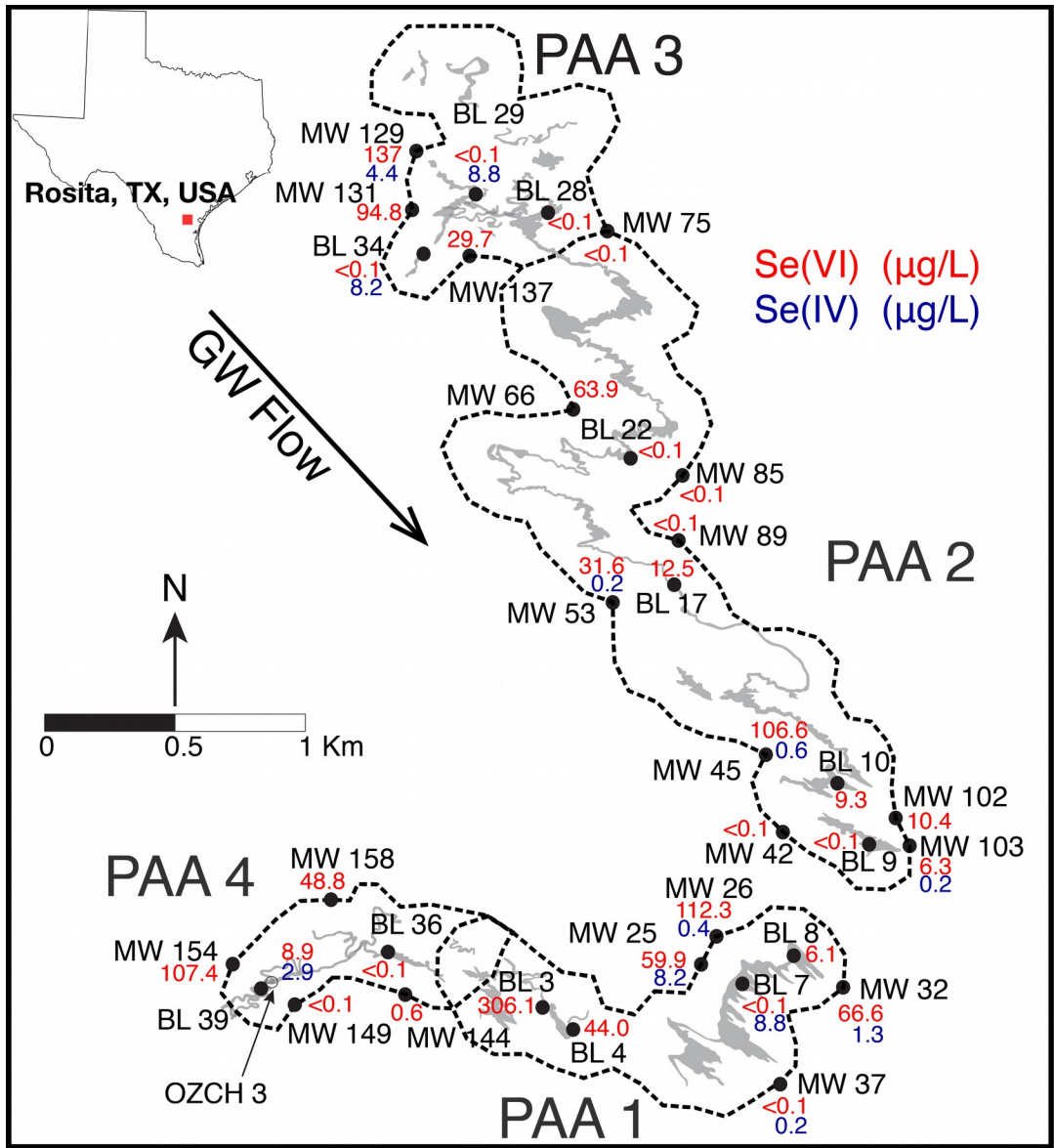
Depth b.g.s (m)	Se (µg/kg)	δ⁸²Se
60.66 - 60.96 (background)	24.3	-1.54‰
66.14 - 66.45	36.8	-1.28‰
66.45 - 66.75	33.8	-0.85‰
66.75 - 67.06	30.8	-0.62‰
67.06 - 67.21	31.7	-0.79‰
70.71 - 71.02	47.6	-0.64‰
71.02 - 71.32	39.0	-0.40‰

545



546

547 Figure 1. a) Pourbaix diagram for Se showing the thermodynamic stability of different Se species
 548 in the environment. Total Se concentration is 10^{-6} M. Light blue fields represent aqueous species,
 549 golden field represents solid Se species. Red, green, and blue symbols represent groundwater
 550 from mining units PAA 1, PAA 2, and PAA 3, respectively.



551

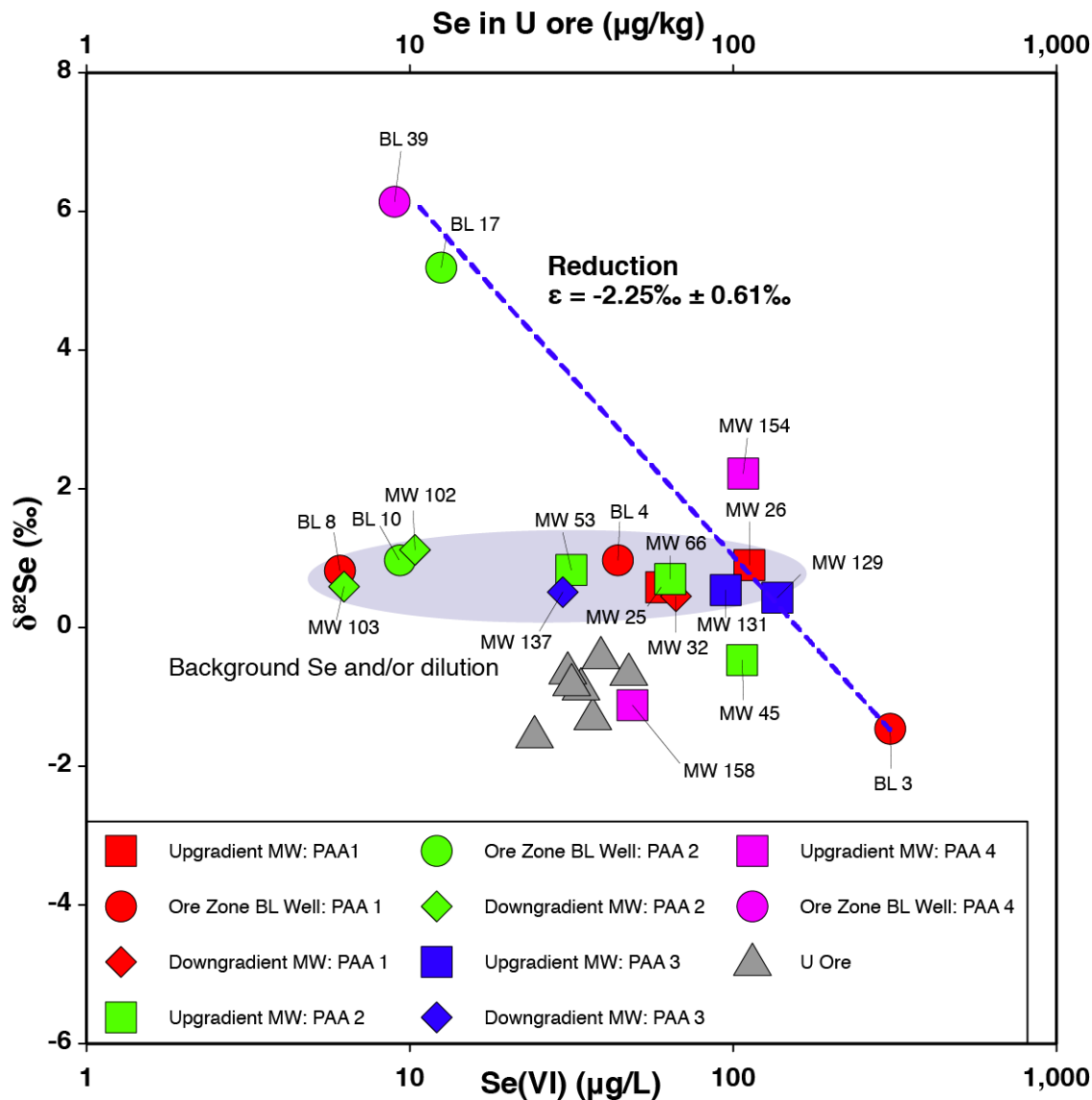
Figu

552re 2. Map of the Rosita ISR site showing the mining units (PAA) and the distribution of Se(VI).

553Light gray areas define the roll-front U deposit. Black dots represent locations of wells sampled

554for Se oxyanion and Se isotope measurements and the open circle shows the location of the

555borehole for the U ore sample. The dotted lines represent the perimeter ring of the monitoring
 556wells. Numbers represent Se-oxyanion concentrations - Se(VI) (red) and Se(IV) (blue) in $\mu\text{g/L}$.



557

558Figure 3. $\delta^{32}\text{Se}$ of aqueous Se(VI) in Rosita groundwater and Se minerals in the U ore vs. Se
 559concentration. Gray triangles represent the U ore and red, green blue and pink symbols represent
 560groundwater from mining units PAA 1, PAA 2, PAA 3, and PAA 4, respectively. The error bars
 561($2 \times \text{s.e.}$) for are smaller than the size of the symbols. The blue dotted line represent the modeled

^{56}Se using a Rayleigh distillation model with $\epsilon = -2.25\text{‰} \pm 0.61\text{‰}$ excluding the samples with $^{56}\text{NO}_3^-$.